A Reversible Silicon–Carbon Bond Cleavage Process. Dynamics and Reactivity of $Cp^*_2Ru_2(\mu\text{-}CH_2)(SiMe_3)(\mu\text{-}Cl)$

Wenbin Lin, Scott R. Wilson, and Gregory S. Girolami*

School of Chemical Sciences, The University of Illinois at Urbana-Champaign, 505 South Mathews Avenue, Urbana, Illinois 61801

Received January 13, 1994®

The methylene/silyl complex $Cp^*_2Ru_2(\mu\text{-}CH_2)(SiMe_3)(\mu\text{-}Cl)$, where $Cp^* = C_5Me_5$, has been prepared by alkylation of $[Cp^*RuCl]_4$ with 1 equiv of $Mg(CH_2SiMe_3)_2$; the product is formed via the unusual cleavage of the α-C—Si bond of the alkyl group. The presence of a bridging methylene ligand and a terminal trimethylsilyl ligand has been demonstrated by ^1H and ^{13}C NMR spectroscopy and confirmed by an X-ray single crystal structure determination. Variable-temperature NMR spectroscopy shows that this molecule undergoes two dynamic processes: the lower temperature process ($\Delta H^\ddagger = 9.0 \pm 0.2$ kcal mol^{-1}, $\Delta S^\ddagger = 0.5 \pm 0.8$ cal mol^{-1} K^{-1}) involves hopping of the silyl ligand between the two ruthenium centers, whereas the higher temperature process ($\Delta H^\ddagger = 12.0 \pm 0.3$ kcal mol^{-1}, $\Delta S^\ddagger = -7 \pm 1$ cal mol^{-1} K^{-1}) involves the reversible re-formation of the C—Si bond between the silyl and methylene ligands. Further evidence that the C—Si bond can be re-formed rests on the observation that treatment of $Cp^*_2Ru_2(\mu\text{-}CH_2)(SiMe_3)(\mu\text{-}Cl)$ with PMe_3 or CO instantly gives the mononuclear Ru^{II} products $Cp^*Ru(CH_2SiMe_3)L_2$ (**2**) and Cp^*RuClL_2 (**3**), in essentially quantitative yield. Protonation of $Cp^*_2Ru_2(\mu\text{-}CH_2)(SiMe_3)(\mu\text{-}Cl)$ with HO_2CCF_3 at low temperature gives the new alkylidene complex $Cp^*_2Ru_2(\mu\text{-}CH_2)(\mu\text{-}O_2CCF_3)(\mu\text{-}Cl)$ (**4**), while protonation of **1** with HO_2CCF_3 at room temperature gives a mixture of **4** and the different alkylidene complex $Cp^*_2Ru_2(\mu\text{-}CHSiMe_3)(\mu\text{-}O_2CCF_3)(\mu\text{-}Cl)$ (**5**), which evidently results from C–Si bond re-formation in **1**. Deuterium labeling studies show that protonation of **1** occurs at a ruthenium center and not at the methylene carbon. Treatment of **4** and **5** with PMe_3 yields the cationic alkylidene complexes $[Cp^*_2Ru_2(\mu\text{-}CH_2)(PMe_3)(\mu\text{-}Cl)][O_2CCF_3]$ (**6**) and $[Cp^*_2Ru_2(\mu\text{-}CHSiMe_3)(PMe_3)(\mu\text{-}Cl)][O_2CCF_3]$ (**7**), respectively. Crystal data for **1**: monoclinic, space group $P2_1/c$, with $a = 10.373(3)$ Å, $b = 14.896(4)$ Å, $c = 17.508(9)$ Å, $\beta = 104.36(4)°$, $V = 2621(3)$ Å^3, $Z = 4$, $R_F = 0.044$, and $R_{wF} = 0.049$ for 254 variables and 2707 data with $I > 2.58\sigma(I)$.

Introduction

The activation of C—H and C—C bonds by transition-metal complexes is of great interest.[1-5] Occasionally, these C—H and C—C bond cleavage processes are chemically reversible: for example, examples of reversible β-hydrogen elimination reactions,[6-8] reversible α-hydrogen eliminations,[8-14] and reversible β-alkyl elimination reactions[15-20] are known. In contrast, there are relatively few examples of silyl elimination reactions where C—Si bonds are broken and the silyl group migrates to a transition-metal center; most of the known examples of such reactions are irreversible processes.[21-25]

Transition-metal-promoted α-silyl elimination reactions are very rare. The first example of such a process was found in derivatives of the Pt(dtbpm) fragment (dtbpm = bis(di-*tert*-butylphosphino)methane), which is able to cleave the C—Si bond of $SiMe_4$ to give $PtMe(SiMe_3)(dtbpm)$.[21] This latter alkyl/silyl species is in slow equilibrium with the alkyl/hydride complex $PtH(CH_2SiMe_3)(dtbpm)$, and the authors proposed that this equilibrium process is intramolecular and involves both α-silyl and α-hydrogen elimination steps. One example of the *opposite* of an α-silyl elimination has recently been

* Abstract published in *Advance ACS Abstracts*, April 15, 1994.

(1) Brookhart, M.; Green, M. L. H.; Wong, L.-L. *Prog. Inorg. Chem.* **1988**, *36*, 1–124.
(2) Shilov, A. E. *Activation of Saturated Hydrocarbons by Transition Metal Complexes*; D. Reidel: Boston, 1984.
(3) Crabtree, R. H.; Hamilton, D. G. *Adv. Organomet. Chem.* **1988**, *28*, 299–338.
(4) Crabtree, R. H. *Chem. Rev.* **1985**, *85*, 245–269.
(5) Bishop, K. C. *Chem. Rev.* **1976**, *76*, 461–486.
(6) Werner, H.; Feser, R. *Angew. Chem., Int. Ed. Engl.* **1979**, *18*, 157–158.
(7) Doherty, N. M.; Bercaw, J. E. *J. Am. Chem. Soc.* **1985**, *107*, 2670–2682.
(8) Fellmann, J. D.; Schrock, R. R.; Traficante, D. D. *Organometallics* **1982**, *1*, 481–484.
(9) Calvert, R. B.; Shapley, J. R. *J. Am. Chem. Soc.* **1977**, *99*, 5225–5226.
(10) Cooper, N. J.; Green, M. L. H. *J. Chem Soc., Dalton Trans.* **1979**, 1121–1127.
(11) Canestrari, M.; Green, M. L. H. *J. Chem. Soc., Dalton Trans.* **1982**, 1789–1793.
(12) Crocker, C.; Empsall, H. D.; Errington, R. J.; Hyde, E. M.; McDonald, W. S.; Markham, M.; Norton, M. C.; Shaw, B. L.; Weeks, B. *J. Chem. Soc., Dalton Trans.* **1982**, 1217–1224.
(13) Turner, H. W.; Schrock, R. R.; Fellmann, J. D.; Holmes, S. J. *J. Am. Chem. Soc.* **1983**, *105*, 4942–4950.
(14) Asselt, A. V.; Burger, B. J.; Gibson, V. C.; Bercaw, J. E. *J. Am. Chem. Soc.* **1986**, *108*, 5347–5349.
(15) Benfield, F. W. S.; Green, M. L. H. *J. Chem. Soc., Dalton Trans.* **1974**, 1324–1331.
(16) Watson, P. L.; Roe, D. C. *J. Am. Chem. Soc.* **1982**, *104*, 6471–6473.
(17) Suggs, J. W.; Cox, S. D. *J. Am. Chem. Soc.* **1984**, *106*, 3054–3056.
(18) Flood, T. C.; Statler, J. A. *Organometallics* **1984**, *3*, 1795–1803.
(19) Crabtree, R. H.; Dion, R. P.; Gibboni, D. J.; McGrath, D. V.; Holt, E. M. *J. Am. Chem. Soc.* **1986**, *108*, 7222–7227.
(20) Bunel, E.; Burger, B. J.; Bercaw, J. E. *J. Am. Chem. Soc.* **1988**, *110*, 976–978.
(21) Hofmann, P.; Heiss, H.; Neiteler, P.; Muller, G.; Lachmann, J. *Angew. Chem., Int. Ed. Engl.* **1990**, *29*, 880–882. See also: Sakaki, S.; Ieki, M. *J. Am. Chem. Soc.* **1993**, *115*, 2373–2381.
(22) Berry, D. H.; Koloski, T. S.; Carroll, P. J. *Organometallics* **1990**, *9*, 2952–2962.
(23) Wakatsuki, Y.; Yamazaki, H.; Nakano, M.; Yamamoto, Y. *J. Chem. Soc., Chem. Commun.* **1991**, 703–704.
(24) Thomson, S. K.; Young, G. B. *Organometallics* **1989**, *8*, 2068–2070.
(25) Koloski, T. S.; Carroll, P. J.; Berry, D. H. *J. Am. Chem. Soc.* **1990**, *112*, 6405–6406.

0276-7333/94/2313-2309$04.50/0

observed: an irreversible migration of a di-*tert*-butylsilyl group from a tantalum center to a methylene carbon.[22]

A few examples of the activation of C–Si bonds by mechanisms other than α-silyl eliminations are known. For example, there is one report of an irreversible β-silyl elimination reaction: $RuHCl(CO)(PPh_3)_2$ reacts with $CH_2{=}CHSiMe_2R$ (R = Me, OEt) to afford $Ru(SiMe_2R)Cl(CO)(PPh_3)_2$ and $CH_2{=}CH_2$ via a $Ru(CH_2CH_2SiMe_2R)Cl(CO)(PPh_3)_2$ intermediate.[23] Finally, there are two examples of β-alkyl eliminations from silicon centers where a metal–silene species is formed; these reactions can be thought of as involving the oxidative addition of a Si—C bond to the metal center. Thermolysis of *cis*-$Pt(CH_2SiMe_3)_2L_2$ (L = PEt_3, PPh_2Me, PPh_3) gives *cis*-$PtMe(CH_2SiMe_2CH_2SiMe_3)L_2$ via a $PtMe(CH_2{=}SiMe_2)(CH_2SiMe_3)L$ intermediate.[24] Similarly, removal of the ethylene ligand from $CpW(\eta^4{:}\eta^1\text{-}C_5H_5SiMe_2CH_2)(C_2H_4)$ yields the tungsten silene complex $Cp_2W(\eta^2\text{-}Me_2Si{=}CH_2)$.[25] This β-alkyl elimination can also be viewed as an α-silyl elimination, depending on whether the silicon or the carbon is considered to be the migrating atom.

In addition to the above interconversions, there are numerous reactions in which C—Si bonds of ligands attached to transition-metal centers are cleaved but which strictly are not elimination reactions because a metal–silicon bond is never formed. Among these are protodesilylation reactions,[26–28] halodesilylation reactions,[29,30] and 1,2-silyl shifts.[26,31,32] The cleavage of carbon–silicon bonds in unactivated tetraalkylsilanes by electrophilic reagents (especially main-group species) has also been utilized in organic syntheses.[33]

We now describe a unique case of a reversible α-C—Si bond cleavage process that is fast on the NMR time scale. This reaction involves the elimination of an α-silyl group from a CH_2SiMe_3 ligand to give a methylene/silyl product. We also describe the reactivity of this unusual methylene/silyl species toward Lewis bases and protonic acids. Among the new species we have isolated from these reactions is a series of new bridging alkylidene complexes; a preliminary version of this work has appeared.[34]

Results and Discussion

Synthesis of the Methylene/Silyl Complex $Cp^*_2Ru_2(\mu\text{-}CH_2)(SiMe_3)(\mu\text{-}Cl)$ by Activation of a CH_2SiMe_3 Ligand. The title compound, a diruthenium bridging methylene/silyl complex, has been prepared in a rather unusual way. Treatment of (pentamethylcyclopentadienyl)ruthenium chloride, $[Cp^*RuCl]_4$,[35–38] with 1 equiv of

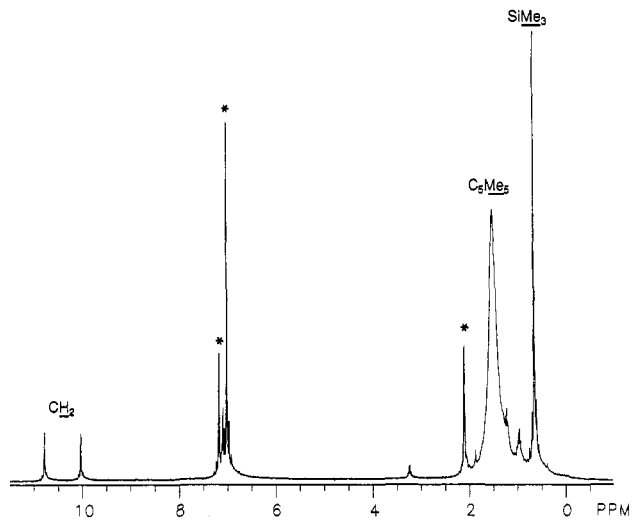

Figure 1. 300-MHz ^1H NMR spectrum of 1 in toluene-d_8 at −80 °C. Asterisks indicate peaks due to residual solvent protons.

$Mg(CH_2SiMe_3)_2$ per tetramer in diethyl ether at 25 °C affords a dark red solution, from which dark red crystals may be isolated. Although the product has the stoichiometry $Cp^*_2Ru_2(CH_2SiMe_3)Cl$, we will show that it is in fact the bridging methylene/silyl complex **1**.[39,40] See Tables

$$[Cp^*RuCl]_4 + Mg(CH_2SiMe_3)_2 \longrightarrow 2\ Cp^*(CH_2)(SiMe_3)Ru{=}Ru(Cl)Cp^* + MgCl_2$$

1

1 and 2 for physical and spectroscopic data for the new compounds described in this paper.

The ^1H NMR spectrum of 1 at −80 °C shows two downfield singlets at δ 10.77 and 10.01 for the methylene protons, a singlet at δ 0.64 for the protons of the trimethylsilyl ligand, and a broad peak centered at δ 1.49 for the protons of the pentamethylcyclopentadienyl groups (Figure 1). The methylene carbon resonance appears at δ 170 as a triplet ($^1J_{CH}$ = 138 Hz) in the ^{13}C NMR spectrum at −80 °C. The ^{13}C NMR spectrum at −80 °C also contains a singlet due to the $SiMe_3$ ligand at δ 6.8 and two sets of signals due to the inequivalent Cp* groups (the quaternary carbons appear at δ 94.6 and 81.6, while the methyl carbons appear at δ 10.2).

The solid-state CPMAS ^{13}C NMR spectrum of 1 at room temperature (Figure 2) is consistent with the low-temperature solution NMR spectrum. Interestingly, the methylene carbon resonance appears as a very broad peak centered at δ 180 (fwhm = 4000 Hz); studies of other bridging methylene complexes have shown that the chemical shift anisotropies of such carbon nuclei are very large.[41] The spectrum also contains resonances for the

(26) Allen, S. R.; Green, M.; Orpen, A. G.; Williams, I. D. *J. Chem. Soc., Chem. Commun.* **1982**, 826–828.
(27) Carmona, E.; Sanchez, L.; Marin, J. M.; Poveda, M. L.; Atwood, J. L.; Priester, R. D.; Rogers, R. D. *J. Am. Chem. Soc.* **1984**, *106*, 3214–3222.
(28) Chang, L. S.; Johnson, M. P.; Fink, M. J. *Organometallics* **1991**, *10*, 1219–1221.
(29) Itoh, K.; Fukahori, T. *J. Organomet. Chem.* **1988**, *349*, 227–234.
(30) Horton, A. D.; Orpen, A. G. *Organometallics* **1992**, *11*, 1193–1201.
(31) Sakurai, H.; Fuji, T.; Sakamoto, K. *Chem. Lett.* **1992**, 339–342 and references therein.
(32) Simpson, S. J.; Andersen, R. A. *J. Am. Chem. Soc.* **1981**, *103*, 4063–4066 and references therein.
(33) Kakiuchi, F.; Furuta, K.; Murai, S.; Kawasaki, Y. *Organometallics* **1993**, *12*, 15–16 and references therein.
(34) Lin, W.; Wilson, S. R.; Girolami, G. S. *J. Am. Chem. Soc.* **1993**, *115*, 3022–3023.
(35) Tilley, T. D.; Grubbs, R. H.; Bercaw, J. E. *Organometallics* **1984**, *3*, 274–278.
(36) Oshima, N.; Suzuki, H.; Moro-oka, Y. *Chem. Lett.* **1984**, 1161–1164.
(37) Fagan, P. J.; Ward, M. D.; Calabrese, J. C. *J. Am. Chem. Soc.* **1989**, *111*, 1698–1719.
(38) Fagan, P. J.; Mahoney, W. S.; Calabrese, J. C.; Williams, I. D. *Organometallics* **1990**, *9*, 1843–1852.
(39) Herrmann, W. A. *Adv. Organomet. Chem.* **1982**, *102*, 209–215 and references therein.
(40) Crabtree, R. H. *The Organometallic Chemistry of the Transition Metals;* Wiley: New York, **1988**; pp 248–259.
(41) Kim, A. J.; Altbach, M. I.; Butler, L. G. *J. Am. Chem. Soc.* **1991**, *113*, 4831–4838.

Table 1. Physical Data for the New Ruthenium Complexes

cmpd	mp (°C)	anal. found (calcd) (%) C	H	Cl	Ru	X
$Cp^*_2Ru_2(\mu\text{-}CH_2)(SiMe_3)(\mu\text{-}Cl)$ (**1**)	160 (dec)	48.7 (48.5)	7.07 (6.90)	5.87 (5.97)	33.9 (34.0)	4.45[b] (4.71)[b]
$Cp^*Ru(PMe_3)_2(CH_2SiMe_3)$ (**2a**)	209 (dec)	50.3 (50.5)	9.23 (9.32)		20.7 (21.2)	12.2[a] (13.0)[a]
$Cp^*Ru(CO)_2(CH_2SiMe_3)$ (**2b**)	91–94	50.6 (50.6)	6.92 (6.90)			
$Cp^*Ru(PMe_3)_2Cl$ (**3a**)	235–239	45.8 (45.3)	7.97 (7.85)	7.02 (8.36)	23.0 (23.8)	12.4[a] (14.6)[a]
$Cp^*Ru(CO)_2Cl$ (**3b**)	144.5–145.5	43.8 (44.0)	4.67 (4.61)	10.1 (10.8)	30.9 (30.8)	
$Cp^*_2Ru_2(\mu\text{-}CH_2)(\mu\text{-}O_2CCF_3)(\mu\text{-}Cl)$ (**4**)	180 (dec)	43.7 (43.5)	5.33 (5.08)	6.01 (5.58)	31.2 (31.8)	
$Cp^*_2Ru_2(\mu\text{-}CHSiMe_3)(\mu\text{-}O_2CCF_3)(\mu\text{-}Cl)$ (**5**)	201.5–202	44.4 (44.1)	5.76 (5.70)	5.07 (5.01)	28.9 (28.6)	3.70[b] (3.97)[b]
$[Cp^*_2Ru_2(\mu\text{-}CH_2)(\mu\text{-}Cl)(PMe_3)][H(O_2CCF_3)_2]$ (**6′**)	106–108	41.0 (40.8)	5.23 (5.13)	4.56 (4.30)	23.8 (24.5)	3.27[a] (3.75)[a]
$[Cp^*_2Ru_2(\mu\text{-}CHSiMe_3)(\mu\text{-}Cl)(PMe_3)][H(O_2CCF_3)_2]$ (**7′**)	168–171	41.4 (41.5)	5.67 (5.62)	3.89 (3.95)	21.0 (22.5)	3.26[a] (3.45)[a]

[a] Phosphorus. [b] Silicon.

Table 2. ^1H and ^{13}C NMR Spectroscopic Data for the New Ruthenium Complexes[a]

cmpd	^1H	assignt	^{13}C or $^{13}C\{^1H\}$
$Cp^*_2Ru_2(\mu\text{-}CH_2)(SiMe_3)(\mu\text{-}Cl)$ (**1**)	10.77 (s)	CH_2	170.0 (t, $^1J_{CH}$ = 138)
	10.01 (s)	CH_2	
		C_5Me_5	94.6 (s)
		C_5Me_5	81.6 (s)
	1.49 (br)	C_5Me_5	10.2 (q, $^1J_{CH}$ = 127)
	0.64 (s)	$SiMe_3$	6.8 (q, $^1J_{CH}$ = 127)
$Cp^*Ru(PMe_3)_2(CH_2SiMe_3)$ (**2a**)		C_5Me_5	89.6 (s)
	1.11 ("t", $^2J_{HP} + {}^4J_{HP}$ = 7.2)	PMe_3	21.8 ("t", $^1J_{CP} + {}^3J_{CP}$ = 25.0)
	1.67 (t, $^4J_{HP}$ = 1.2)	C_5Me_5	11.8 (t, $^2J_{CP}$ = 2.6)
	0.39 (s)	CH_2SiMe_3	5.6 (s)
	–0.99 (t, $^3J_{HP}$ = 6.3)	CH_2SiMe_3	–22.8 (t, $^2J_{CP}$ = 10.5)
$Cp^*Ru(CO)_2(CH_2SiMe_3)$ (**2b**)	1.47 (s)	C_5Me_5	
	0.39 (s)	CH_2SiMe_3	
	–0.33 (s)	CH_2SiMe_3	
$Cp^*Ru(PMe_3)_2Cl$ (**3a**)		C_5Me_5	105.5 (s)
	1.22 ("t", $^2J_{HP} + {}^4J_{HP}$ = 8.4)	PMe_3	20.4 ("t", $^1J_{CP} + {}^3J_{CP}$ = 25.2)
	1.57 (t, $^4J_{HP}$ = 1.5)	C_5Me_5	11.0 (s)
$Cp^*Ru(CO)_2Cl$ (**3b**)	1.37 (s)	C_5Me_5	
$Cp^*_2Ru_2(\mu\text{-}CH_2)(\mu\text{-}O_2CCF_3)(\mu\text{-}Cl)$ (**4**)	11.22 (d, $^2J_{HH}$ = 0.8)	CH_2	177.3 (s)
	9.55 (d, $^2J_{HH}$ = 0.8)	CH_2	
		C_5Me_5	87.2 (s)
	1.62 (s)	C_5Me_5	10.3 (s)
$Cp^*_2Ru_2(\mu\text{-}CHSiMe_3)(\mu\text{-}O_2CCF_3)(\mu\text{-}Cl)$ (**5**)	13.45 (s)	$CHSiMe_3$	195.3 (d, $^1J_{CH}$ = 120)
		CO_2CF_3	164.5 (q, $^2J_{CF}$ = 37)
		CO_2CF_3	113.0 (q, $^1J_{CF}$ = 288)
		C_5Me_5	87.5 (s)
	1.60 (s)	C_5Me_5	10.9 (q, $^1J_{CH}$ = 127)
	0.03 (s)	$CHSiMe_3$	5.0 (q, $^1J_{CH}$ = 118)
$[Cp^*_2Ru_2(\mu\text{-}CH_2)(\mu\text{-}Cl)(PMe_3)][X]$ (**6**)[b]	10.88 (t, $^2J_{HH} = {}^3J_{PH}$ = 3.5)	CH_2	176.0 (d, $^2J_{CP}$ = 10.7)
	9.83 (dd, $^2J_{HH}$ = 3.5, $^3J_{PH}$ = 18.5)	CH_2	
		C_5Me_5	98.2 (d, $^2J_{CP}$ = 2.4)
		C_5Me_5	85.2 (s)
	1.17 (d, $^2J_{HP}$ = 9.5)	PMe_3	18.3 (d, $^1J_{CP}$ = 30.8)
	1.65 (d, $^4J_{HP}$ = 1.5)	C_5Me_5	11.1 (s)
	1.64 (s)	C_5Me_5	10.0 (s)
$[Cp^*_2Ru_2(\mu\text{-}CHSiMe_3)(\mu\text{-}Cl)(PMe_3)][X]$ (**7**)[b]	13.15 (d, $^3J_{HP}$ = 18.5)	$CHSiMe_3$	202.9 (d, $^2J_{CP}$ = 4.7)
		C_5Me_5	97.7 (d, $^2J_{CP}$ = 2.6)
		C_5Me_5	86.1 (s)
	1.18 (d, $^2J_{HP}$ = 9.0)	PMe_3	21.3 (d, $^1J_{CP}$ = 28.7)
	1.64 (s)	C_5Me_5	12.0 (s)
	1.61 (d, $^4J_{HP}$ = 1.8)	C_5Me_5	10.6 (s)
	0.03 (s)	$CHSiMe_3$	7.0 (s)

[a] For compound **1**, the ^1H and $^{13}C\{^1H\}$ NMR spectra were taken at –80 °C in C_7D_8 and CD_2Cl_2, respectively. All other NMR spectra were taken at 25 °C in the following solvents: C_6D_6 (**2a,b** and **3a,b**), CD_2Cl_2 (**4–7**). All chemical shifts are in ppm, and all J values are in Hz. [b] X = O_2CCF_3 or $[H(O_2CCF_3)_2]$.

inequivalent Cp* groups (δ 96.0, 81.8, 12.1, and 10.6) and a resonance for the trimethylsilyl group at δ 9.2.

The dynamic behavior of **1** in solution will be discussed after its molecular structure has been described.

X-ray Crystal Structure of 1. Single crystals of **1**, grown from pentane at –25 °C, crystallize in the monoclinic space group $P2_1/n$ with four molecules in the unit cell. One molecule, which resides on a general position, is present in the asymmetric unit. Crystal data are presented in Table 3, atomic coordinates are listed in Table 4, and

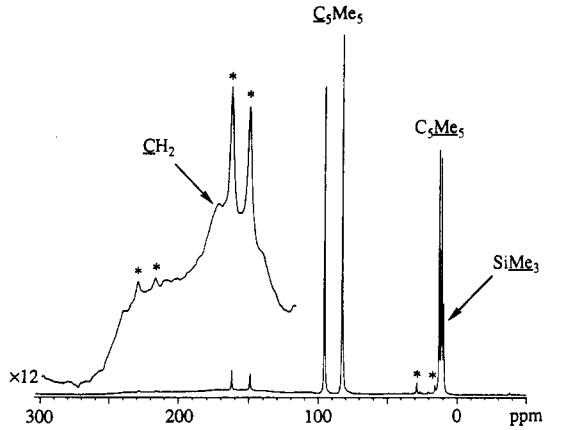

Figure 2. 75-MHz CP MAS ^{13}C NMR spectrum of 1 at 25 °C. Asterisks indicate spinning sidebands. The broad feature between δ 200 and 250 is a spinning sideband of the CH_2 resonance at δ 170.

Table 3. Crystal Data for $Cp^*_2Ru_2(\mu\text{-}CH_2)(SiMe_3)(\mu\text{-}Cl)$ (1)

space group: $P2_1/n$	T = −75 °C
a = 10.373(4) Å	Z = 4
b = 14.896(4) Å	mol wt: 595.27
c = 17.508(9) Å	d_{calcd} = 1.508 g cm^{-3}
β = 104.36(4)°	μ_{calcd} = 12.87 cm^{-1}
V = 2621(3) Å^3	size: 0.1 × 0.2 × 0.2 mm

diffractometer: Enraf-Nonius CAD4
radiation: Mo K$\bar{\alpha}$, $\bar{\lambda}$ = 0.710 73 Å
monochromator: graphite crystal, 2θ = 12°
scan range, type: $2.0 < 2\theta < 48.0°$, ω/θ
scan speed, width: 3–16° min^{-1}, $\Delta\omega = 1.50[1.10 + 0.35 \tan\theta]$°
no. of rflns: 4524 total, 4096 unique, 2707 with $I > 2.58\sigma(I)$
internal consistency: R_i = 0.025

R_F = 0.044	variables: 254
R_{wF} = 0.049	p factor: 0.020

Table 4. Atomic Coordinates for $Cp^*_2Ru_2(\mu\text{-}CH_2)(SiMe_3)(\mu\text{-}Cl)$ (1)

	x/a	y/b	z/c
Ru(1)	0.11656(6)	0.27734(5)	0.91056(4)
Ru(2)	0.12635(6)	0.37619(4)	0.79486(4)
Cl	0.0732(2)	0.2213(2)	0.7790(1)
Si	−0.1179(2)	0.2901(2)	0.8951(2)
C(1)	0.1494(8)	0.2031(6)	1.0261(5)
C(2)	0.2252(8)	0.2843(6)	1.0365(5)
C(3)	0.3240(7)	0.2757(6)	0.9934(5)
C(4)	0.3036(7)	0.1944(5)	0.9512(5)
C(5)	0.1942(8)	0.1494(6)	0.9713(5)
C(6)	0.0534(10)	0.1747(8)	1.0740(6)
C(7)	0.222(1)	0.3559(7)	1.0968(6)
C(8)	0.4331(9)	0.3432(6)	0.9944(6)
C(9)	0.3827(9)	0.1570(7)	0.8988(6)
C(10)	0.143(1)	0.0568(6)	0.9441(7)
C(11)	0.2341(8)	0.4954(6)	0.7833(5)
C(12)	0.0941(8)	0.5124(6)	0.7530(5)
C(13)	0.0476(8)	0.4524(6)	0.6871(5)
C(14)	0.1566(9)	0.4024(6)	0.6753(5)
C(15)	0.2714(8)	0.4270(6)	0.7373(5)
C(16)	0.3252(9)	0.5478(6)	0.8472(6)
C(17)	0.0142(10)	0.5826(6)	0.7818(6)
C(18)	−0.0928(8)	0.4505(7)	0.6345(6)
C(19)	0.155(1)	0.3340(7)	0.6154(6)
C(20)	0.4086(9)	0.3895(8)	0.7472(6)
C(21)	−0.2110(9)	0.3517(8)	0.8040(7)
C(22)	−0.1723(9)	0.3497(7)	0.9773(7)
C(23)	−0.2038(10)	0.1781(7)	0.8852(7)
C(24)	0.1096(9)	0.4135(6)	0.9057(5)

selected bond distances and angles are collected in Table 5.

In agreement with the NMR data, molecules of 1 consist of two ruthenium centers that are bridged by a methylene group and a chloride atom (Figure 3). Each ruthenium atom is η^5-bonded to a pentamethylcyclopentadienyl group; the ruthenium–centroid distances of 1.896(8) Å to Ru(1) and 1.795(9) Å to Ru(2) are significantly different and reflect the different coordination numbers of the two metal centers: the longer Ru–centroid distance is seen for the ruthenium atom with the higher coordination number.

The trimethylsilyl group is terminal on Ru(1), and the Ru—Si distance of 2.387(2) Å is at the low end of the 2.34–2.57-Å range observed for Ru—Si single bonds in other complexes.[42] The relatively short Ru—Si distance

Table 5. Bond Distances and Angles for $Cp^*_2Ru_2(\mu\text{-}CH_2)(SiMe_3)(\mu\text{-}Cl)$ (1)

Bond Distances (Å)

Ru(1)–Ru(2)	2.527(1)	C(1)–C(5)	1.41(1)
Ru(1)–Cl	2.386(2)	C(2)–C(3)	1.42(1)
Ru(2)–Cl	2.373(2)	C(3)–C(4)	1.41(1)
Ru(1)–Si	2.387(2)	C(4)–C(5)	1.43(1)
Ru(1)–C(24)	2.030(8)	C(1)–C(6)	1.51(1)
Ru(2)–C(24)	2.066(9)	C(2)–C(7)	1.51(1)
Ru(1)–C(1)	2.257(9)	C(3)–C(8)	1.51(1)
Ru(1)–C(2)	2.216(8)	C(4)–C(9)	1.48(1)
Ru(1)–C(3)	2.277(8)	C(5)–C(10)	1.51(1)
Ru(1)–C(4)	2.261(8)	C(11)–C(12)	1.44(1)
Ru(1)–C(5)	2.233(9)	C(11)–C(15)	1.41(1)
Ru(2)–C(11)	2.135(8)	C(12)–C(13)	1.44(1)
Ru(2)–C(12)	2.155(9)	C(13)–C(14)	1.41(1)
Ru(2)–C(13)	2.179(9)	C(14)–C(15)	1.44(1)
Ru(2)–C(14)	2.227(9)	C(11)–C(16)	1.49(1)
Ru(2)–C(15)	2.146(9)	C(12)–C(17)	1.50(1)
Si–C(21)	1.88(1)	C(13)–C(18)	1.52(1)
Si–C(22)	1.89(1)	C(14)–C(19)	1.46(1)
Si–C(23)	1.88(1)	C(15)–C(20)	1.50(1)
C(1)–C(2)	1.43(1)		

Bond Angles (deg)

Ru(1)–Ru(2)–C(24)	51.3(2)	Cl–Ru(2)–C(24)	107.5(2)
Ru(2)–Ru(1)–C(24)	52.6(3)	Cl–Ru(1)–Cp(1)	122.3(3)
Ru(2)–Ru(1)–Si	96.02(7)	Cl–Ru(2)–Cp(2)	131.4(3)
Ru(1)–Ru(2)–Cp(2)	168.1(3)	Cl–Ru(1)–Si	88.58(9)
Ru(2)–Ru(1)–Cp(1)	137.2(2)	Si–Ru(1)–Cp(1)	126.2(3)
Ru(1)–Ru(2)–Cl	58.18(6)	Ru(1)–Si–C(21)	115.4(3)
Ru(2)–Ru(1)–Cl	57.68(6)	Ru(1)–Si–C(22)	116.0(3)
Si–Ru(1)–C(24)	83.8(3)	Ru(1)–Si–C(23)	112.7(3)
Cl–Ru(1)–C(24)	108.2(3)	Ru(1)–Si–C(23)	112.7(3)
Cp(1)–Ru(1)–C(24)	118.8(4)	C(21)–Si–C(22)	103.2(5)
Cp(2)–Ru(2)–C(24)	120.9(4)	C(21)–Si–C(23)	102.8(5)
Ru(1)–C(24)–Ru(2)	76.2(3)	C(22)–Si–C(23)	105.3(5)
Ru(1)–Cl–Ru(2)	64.13(6)		

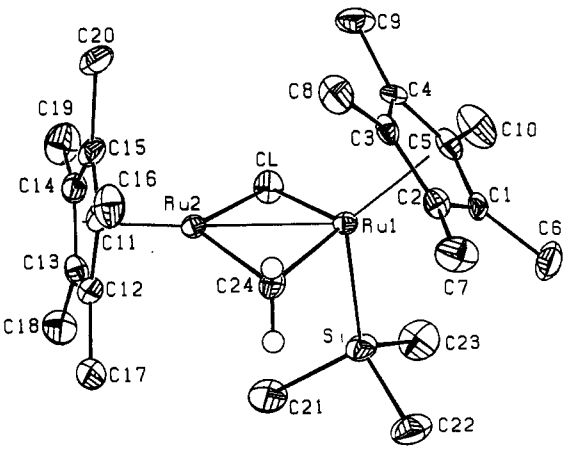

Figure 3. ORTEP diagram of 1. The ellipsoids represent the 35% probability density surfaces.

(42) Straus, D. A.; Zhang, C.; Quimbita, G. E.; Grumbine, S. D.; Heyn, R. H.; Tilley, T. D.; Rheingold, A. L.; Geib, S. J. *J. Am. Chem. Soc.* **1990**, *112*, 2673–2681 and references therein.

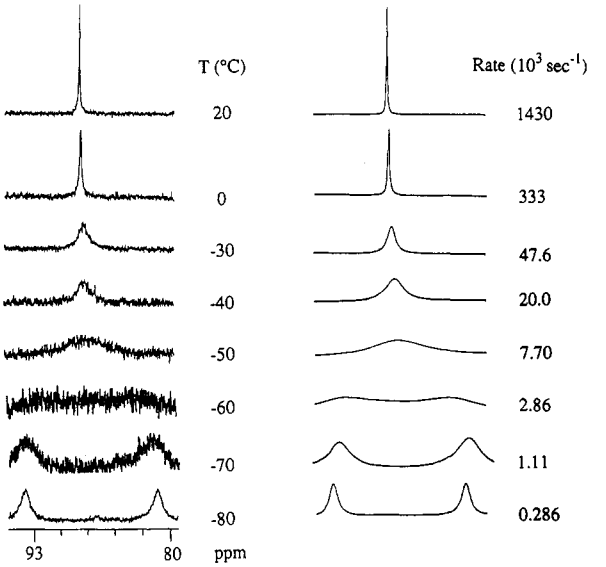

Figure 4. 75-MHz variable-temperature $^{13}C\{^1H\}$ NMR line shapes for the quaternary carbons of the two Cp* groups of 1: (left) experimental spectra; (right) simulated spectra.

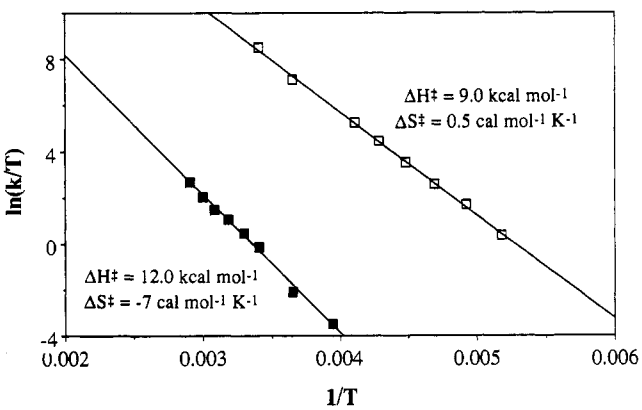

Figure 5. Eyring plots of the two dynamic processes of 1 as deduced from variable-temperature ^1H and $^{13}C\{^1H\}$ NMR spectroscopy.

in 1 probably reflects the presence of significant π back-bonding interactions from filled orbitals on ruthenium to empty Si—C σ^* orbitals on silicon. It is well-known that metal–silicon distances in transition-metal silyl complexes are often shorter than values predicted from single-bond radii because of such $d\pi$–$p\pi$ back-bonding interactions from the metal to silicon.[42,43]

Electron counting suggests that compound 1 contains a Ru=Ru double bond, and, in fact, the Ru–Ru distance of 2.527(1) Å is considerably shorter than the 2.637–2.734-Å range seen for other structurally characterized alkylidene-bridged diruthenium complexes, as shown in Table 6.[44-48] The Ru–Ru distance of 2.527 Å is, in fact, comparable to those of some other diruthenium compounds with Ru=Ru double bonds;[49,50] to our knowledge, 1 contains the first Ru=Ru double bond bridged by an alkylidene ligand.

Correspondingly, the two Ru–C distances to the bridging methylene group in 1, which average 2.048(9) Å, are short relative to those of known diruthenium compounds with bridging methylene groups, and the Ru–C–Ru bond angle of 76.2(3)° is more acute than those of the diruthenium bridging methylene compounds in Table 6.[44-48]

Dynamic Behavior of 1. Silyl Migration Reactions. Although the numbers of resonances seen in the solid state and low-temperature solution NMR spectra are consistent with the crystal structure of 1, the room-temperature NMR spectra reveal that 1 is a dynamic molecule in solution, since only one Cp* resonance is seen and the resonances for the diastereotopic methylene protons are abnormally broad. This has been confirmed by studying the solution ^1H and ^{13}C NMR spectra of $Cp^*_2Ru_2(\mu\text{-}CH_2)(SiMe_3)(\mu\text{-}Cl)$ as a function of temperature.

Compound 1 engages in two separate dynamic processes. The first process effects exchange of the Cp* environments *without* exchanging the diastereotopic protons of the bridging methylene group: the two Cp* ring carbon resonances observed at −80 °C in the $^{13}C\{^1H\}$ NMR spectrum broaden as the temperature is raised and coalesce at −50 °C. The line shapes of the Cp* resonances were compared with computer-generated spectra for a two-site exchange process to obtain the exchange rates as a function of temperature (Figure 4). A least-squares calculation based on the Eyring equation yielded the activation parameters $\Delta H^\ddagger = 9.0 \pm 0.2$ kcal mol^{-1} and $\Delta S^\ddagger = 0.5 \pm 0.8$ cal mol^{-1} K^{-1} for the process that exchanges the two Cp* environments (Figure 5).

Only one reasonable exchange mechanism could render the two Cp* groups equivalent on the NMR time scale without exchanging the two diastereotopic methylene protons, namely, migration of the trimethylsilyl group from one ruthenium center to the other via a symmetric Ru-(μ-$SiMe_3$)Ru intermediate:

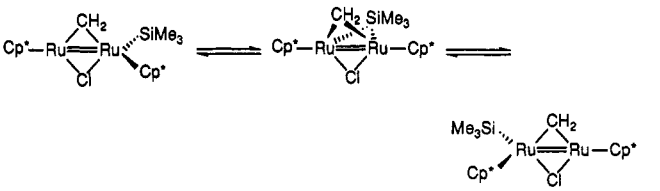

This is the first example of the reversible migration of silyl groups between metal centers. An example of irreversible migration of a trialkylsilyl group between transition-metal centers has recently been reported,[51] and even more recently, a second example of the rapid, reversible migration of a trialkylsilyl group from one metal center to another has been reported by Akita *et al.*: hopping of a $-SiMe_3$ ligand between the two Ru centers in $Cp_2Ru_2(\mu\text{-}CH_2)(CO)_2(SiMe_3)H$.[52]

The second exchange process exhibited by 1 effects the permutation of the two methylene protons: the two methylene ^1H NMR resonances, which are sharp below 0

(43) Tilley, T. D. In *The Chemistry of Organic Silicon Compounds*; Patai, S., Rappoport, Z., Eds.; Wiley: New York, 1989; Chapter 24, p 1415.

(44) Hursthouse, M. B.; Jones, R. A.; Malik, K. M. A.; Wilkinson, G. *J. Am. Chem. Soc.* **1979**, *101*, 4128–4139.

(45) Jones, R. A.; Wilkinson, G.; Galas, A. M. R.; Hursthouse, M. B.; Malik, K. M. A. *J. Chem. Soc., Dalton Trans.* **1980**, 1771–1778.

(46) Davies, D. L.; Knox, S. A. R.; Mead, K. A.; Morris, M. J.; Woodward, P. *J. Chem. Soc., Dalton Trans.* **1984**, 2293–2299.

(47) Colborn, R. E.; Dyke, F. A.; Knox, S. A. R.; Mead, K. A.; Woodward, P. *J. Chem. Soc., Dalton Trans.* **1983**, 2099–2108.

(48) Kakigano, T.; Suzuki, H.; Igarashi, M.; Moro-oka, Y. *Organometallics* **1990**, *9*, 2192–2194.

(49) Eisenberg, R.; Gaughan, A. P., Jr.; Pierpont, C. G.; Reed, J.; Shultz, A. J. *J. Am. Chem. Soc.* **1972**, *94*, 6240–6241.

(50) Jones, R. A.; Wilkinson, G.; Colquohoun, I. J.; McFarlane, W.; Galas, A. M. R.; Hursthouse, M. B. *J. Chem. Soc., Dalton Trans.* **1980**, 2480–2487.

(51) Braunstein, P.; Knorr, M.; Hirle, B.; Reinhard, G.; Schubert, U. *Angew. Chem., Int. Ed. Engl.* **1992**, *31*, 1583–1585.

(52) Akita, M.; Oku, T.; Hua, R.; Moro-oka, Y. *J. Chem. Soc., Chem. Commun.* **1993**, 1670–1672.

Table 6. Comparison of the Structural Parameters of Bridging Methylene Compounds of Ruthenium

cmpd	Ru–Ru (Å)	Ru–C (Å)	Ru–C–Ru (deg)	ref
$Cp^*_2Ru_2(\mu\text{-}CH_2)(SiMe_3)(\mu\text{-}Cl)$	2.527	2.048	76.2	this work
$[Ru_3(\mu\text{-}CH_2)_4(PMe_3)_8][BF_4]_2$	2.637	2.036	80.7	45
$[(PMe_3)_3Ru(\mu\text{-}CH_2)_2Ru(PMe_3)_3][BF_4]_2$	2.641	2.071	79.2	44
$(PMe_3)_3Ru(\mu\text{-}CH_2)_3Ru(PMe_3)_3$	2.650	2.108	78.1	44
cis-$Cp_2Ru_2(CO)_2(\mu\text{-}CO)(\mu\text{-}CH_2)$	2.707	2.078	81.3	46
cis-$Cp_2Ru_2(CO)_2(\mu\text{-}CO)(\mu\text{-}CMe_2)$	2.712	2.088	79.8	47
$[(PMe_3)_3Ru(\mu\text{-}CH_2)_2(\mu\text{-}CH_3)(PMe_3)_3][BF_4]$	2.732	2.108	80.8	44
$[Cp^*_2Ru_2(CO)_2(\mu\text{-}Cl)(\mu\text{-}CH_2)][BF_4]$	2.734	2.113	81.2	48

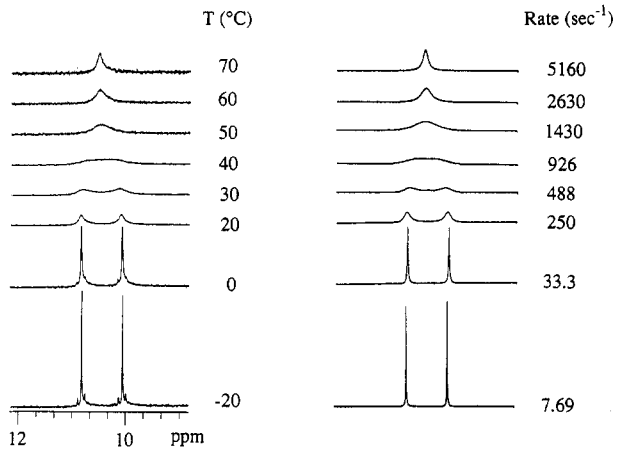

Figure 6. 300-MHz variable-temperature ^1H NMR line shapes for the diastereotopic methylene protons of 1: (left) experimental spectra; (right) simulated spectra.

°C, broaden as the temperature is raised and coalesce at 50 °C (Figure 6). Comparisons with computer-generated spectra for this two-site exchange process yield activation parameters of $\Delta H^\ddagger = 12.0 \pm 0.3$ kcal mol^{-1} and $\Delta S^\ddagger = -7 \pm 1$ cal mol^{-1} K^{-1} (Figure 5). Since the activation parameters for exchange of the Cp* groups and for exchange of the two diastereotopic methylene protons are significantly different, it is clear that 1 undergoes two different fluxional processes in solution.

Several mechanisms can be written that would effect exchange of the diastereotopic methylene protons (Scheme 1). These include breaking of one Ru—C bond and subsequent rotation of a terminal methylene group about its Ru=C axis (mechanism I),[53] rotation around the Ru=Ru bond in a completely unbridged intermediate (mechanism II),[54] swapping of the terminal Cp* and silyl groups on the tetrahedral ruthenium center via a square-planar intermediate (mechanism III), and migration of the trimethylsilyl group to the methylene carbon to reform the C—Si bond (mechanism IV). We will show below that a comparison with a closely related molecule strongly supports mechanism IV and rules out the rest.

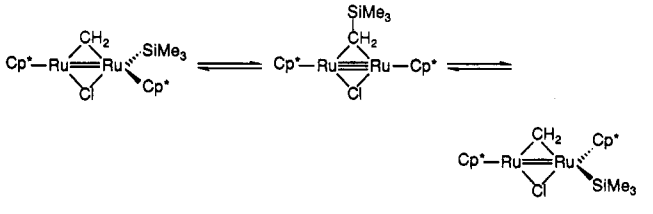

The reversible migration of the trimethylsilyl group to the methylene carbon center does in fact make the two methylene protons equivalent and would be the reverse of the pathway by which (presumably) the methylene/silyl complex is generated from the reactants.

To the best of our knowledge, the high-temperature dynamic process exhibited by 1 is the first example of a *rapid* reversible C—Si bond cleavage/re-formation process in an organotransition-metal complex.[55–58] For comparison, the equilibrium noted in the Introduction between $PtMe(SiMe_3)$(dtbpm) and $PtH(CH_2SiMe_3)$(dtbpm) is *not* fast on the NMR time scale.[21] In two of the C—Si bond cleavage processes discussed in the Introduction, the C—Si bond can be re-formed *chemically*. In the first example, removal of the ethylene ligand from $CpW(\eta^4{:}\eta^1\text{-}C_5H_5SiMe_2CH_2)(C_2H_4)$ yields the tungsten silene complex $Cp_2W(\eta^2\text{-}Me_2Si{=}CH_2)$; readdition of C_2H_4 to the latter compound re-forms the C—Si bond to give $CpW(\eta^4{:}\eta^1\text{-}C_5H_5SiMe_2CH_2)(C_2H_4)$.[25] In the second example, treatment of $Cp'_2Zr[CH(SiMe_3)_2]Cl$ (Cp′ = *rac*-C_2H_4(indenyl)$_2$) with $AlCl_3$ yields $Cp'_2Zr[CH(SiMe_2Cl)SiMe_3]^+$, and the latter reacts with $AlMe_3$ to re-form the C—Si bond and regenerate $Cp'_2Zr[CH(SiMe_3)_2]Cl$.[30] However, both of these C—Si bond cleavage/reformation processes involve the addition of external reagents.

Reactivity of 1 toward Lewis Bases: Re-formation of the C–Si Bond. The variable-temperature NMR spectra suggest that $Cp^*_2Ru_2(\mu\text{-}CH_2)(SiMe_3)(\mu\text{-}Cl)$ undergoes rapid reversible C—Si bond re-formation in solution. We were interested in trapping the product of this C—Si bond re-formation process by chemical means, and we have been able to accomplish this by treatment of 1 with Lewis bases such as PMe_3 and CO. Treatment of 1 with 4 equiv of PMe_3 in diethyl ether gives the known[35] mononuclear Ru^{II} products $Cp^*Ru(CH_2SiMe_3)(PMe_3)_2$, (**2a**) and $Cp^*RuCl(PMe_3)_2$ (**3a**) in quantitative yield.

$$Cp^*_2Ru_2(\mu\text{-}CH_2)(SiMe_3)(\mu\text{-}Cl) + 4L \rightarrow Cp^*Ru(CH_2SiMe_3)L_2 + Cp^*RuClL_2$$
$$\textbf{2a,b} \qquad\qquad \textbf{3a,b}$$

L = PMe_3 (**2a**, **3a**); L = CO (**2b**, **3b**)

Sealed-NMR-tube studies show that this reaction goes to completion instantaneously even at −78 °C. Carbonylation of 1 with 2 atm of CO gives the analogous products $Cp^*Ru(CH_2SiMe_3)(CO)_2$ (**2b**) and $Cp^*RuCl(CO)_2$ (**3b**) in high yield. The (trimethylsilyl)methyl groups in **2a,b** must have been generated by re-formation of the C—Si bond; these results suggest that the methylene/silyl complex 1 is in equilibrium with a second species in which the C—Si bond has re-formed (Scheme 2). Presumably, this second species

(53) Berry, D. H.; Bercaw, J. E. *Polyhedron* **1988**, *7*, 759–766.
(54) Dyke, A. F.; Knox, S. A. R.; Mead, K. A.; Woodward, P. *J. Chem. Soc., Chem. Commun.* **1981**, 861–862.
(55) Rapid reversible C—Si bond cleavage/re-formation processes have been observed in silyl-substituted cyclopentadienes and related indenes.[56–58]
(56) Ashe, A. J. *J. Am. Chem. Soc.* **1970**, *92*, 1233–1235.
(57) Abel, E. W.; Dunster, M. O.; Waters, A. *J. Organomet. Chem.* **1973**, *49*, 287–321.
(58) Ustynyuk, Y. U.; Kisin, A. V.; Pribytkova, I. M.; Zenkin, A. A.; Antonova, N. D. *J. Organomet. Chem.* **1972**, *42*, 47–63.

Scheme 1. Possible Exchange Mechanisms for Permutation of the Diastereotopic Methylene Protons in 1

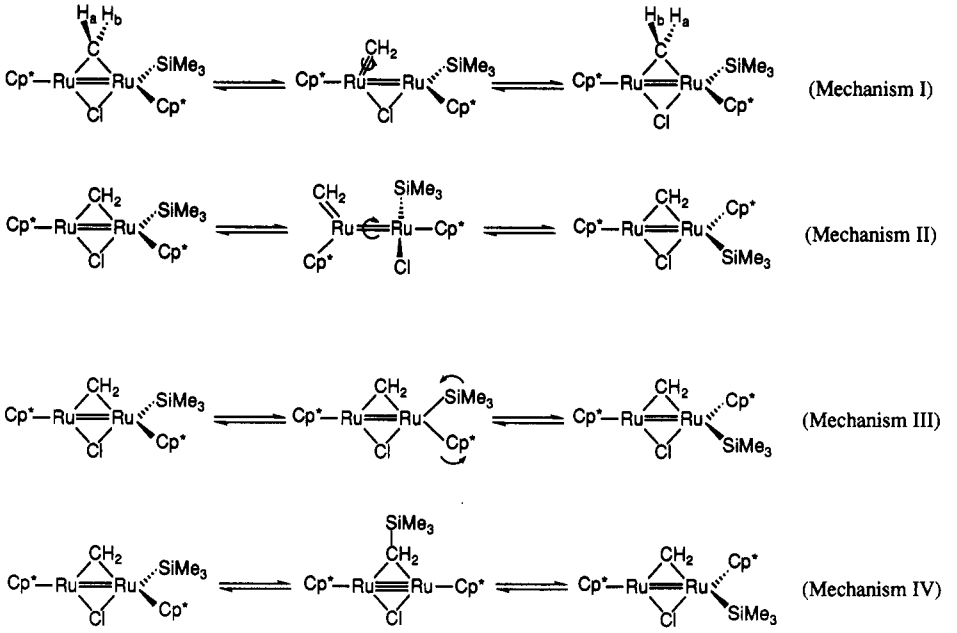

Scheme 2. Proposed Involvement of a (Trimethylsilyl)methyl Intermediate in the Reactions of 1 with Lewis Bases

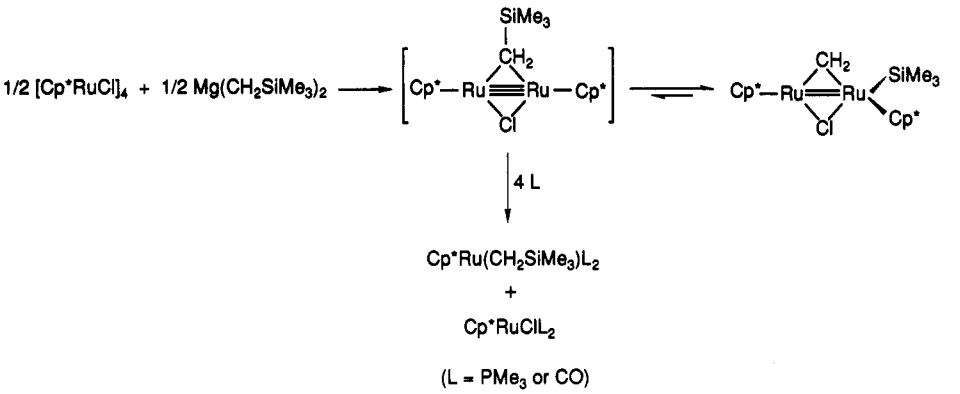

is the (trimethylsilyl)methyl complex $Cp^*_2Ru_2(\mu\text{-}CH_2SiMe_3)(\mu\text{-}Cl)$, which is cleaved by Lewis bases to form **2** and **3**. Alternatively, Lewis bases could attack **1** directly and *promote* the subsequent re-formation of the C—Si bond and cleavage to mononuclear products.

Reactivity of 1 toward Trifluoroacetic Acid: Synthesis of New Bridging Alkylidene Complexes. We have also investigated the reactivity of **1** toward acids. Treatment of **1** with HO_2CCF_3 at low temperatures (−78 °C) followed by warming gives a dark blue product which has been identified as the new bridging methylene complex $Cp^*_2Ru_2(\mu\text{-}CH_2)(\mu\text{-}O_2CCF_3)(\mu\text{-}Cl)$ (**4**). The presence of a Ru—Ru single bond in **4** can be inferred from its diamagnetism.

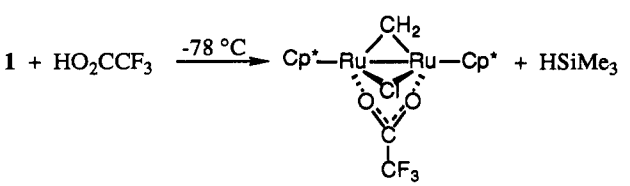

4

Electrical conductivity studies show that **4** is a non-electrolyte in nitrobenzene.[59] The IR spectrum of **4** shows a strong peak at 1642 cm^{-1} due to the antisymmetric CO_2 stretch of the carboxylate group. The position of this band is consistent with the view that the O_2CCF_3 group in **4** is a bridging ligand; other known transition-metal complexes with bridging trifluoroacetate groups have $\nu_{asym}(CO_2)$ stretches between 1600 and 1665 cm^{-1}.[60]

The ^1H NMR spectrum of **4** contains doublets at δ 11.22 and 9.55 for the two inequivalent protons of the bridging methylene; the geminal $^2J_{HH}$ coupling constant is 0.8 Hz. The $^{13}C\{^1H\}$ NMR resonance for the methylene carbon in **4** appears at δ 177.3. The two Cp* groups are equivalent, as shown by the singlets in the ^1H and $^{13}C\{^1H\}$ NMR spectra even at low temperatures. The equivalency of the two Cp* ligands further supports the contention that the two ruthenium centers in **4** are bridged by the methylene, chloride, and trifluoroacetate groups. The iodo analogue of **4** has been prepared by a completely different route.[61]

When **1** is treated with DO_2CCF_3 at low temperatures, essentially no deuterium is incorporated into the methylene unit of the product; this shows that the methylene unit is

(59) Geary, W. J. *Coord. Chem. Rev.* **1972**, *7*, 81–122.
(60) Mehrotra, R. C.; Bohra, R. *Metal Carboxylates*; Academic Press: New York, 1983; pp 54–56.
(61) Suzuki, H.; Kakigano, T.; Igarashi, M.; Tanaka, M.; Moro-oka, Y. *J. Chem. Soc., Chem. Commun.* **1991**, 283–285.

not the site of protonation. Instead, protonation evidently occurs at a ruthenium center and is followed by the rapid reductive elimination of trimethylsilane.

Surprisingly, protonation of **1** with HO_2CCF_3 at room temperature leads to a mixture of **4** and another new bridging alkylidene complex in which the C—Si bond has re-formed, $Cp^*_2Ru_2(\mu\text{-}CHSiMe_3)(\mu\text{-}O_2CCF_3)(\mu\text{-}Cl)$ (**5**).

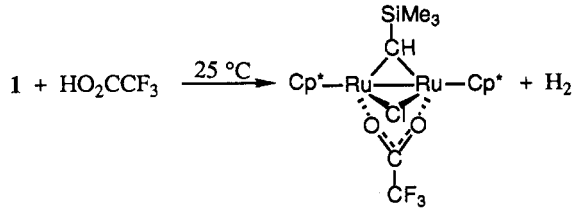

5

Although **4** and **5** are difficult to separate, we found that, by treating a toluene solution of **4** and **5** with PMe_3, the former reacts to form a salt (see below) whereas the latter does not react. Separation of **5** from the PMe_3 adduct of **4** is easily accomplished by crystallization. Sealed-tube NMR studies have confirmed that dihydrogen is evolved when $Cp^*_2Ru_2(\mu\text{-}CH_2)(SiMe_3)(\mu\text{-}Cl)$ is treated with HO_2CCF_3 at room temperature.

In the ^1H NMR spectrum of **5**, the downfield singlet of intensity 1 at δ 13.45 and the singlet of intensity 9 at δ 0.03 are assigned to the protons of a bridging (trimethylsilyl)methylidene group. The ^{13}C NMR spectrum of **5** shows a doublet ($^1J_{CH}$ = 120 Hz) at δ 195.3 for the methylidene carbon. The equivalency of the two Cp* groups in both the ^1H and ^{13}C NMR spectra again suggests that **5** is a diruthenium complex bridged by the (trimethylsilyl)methylidene, trifluoroacetate, and chloride groups. The structure of complex **5** again shows that the C—Si bond in **1** can be re-formed.

We have carried out protonations of **1** with DO_2CCF_3 at room temperature in order to learn more about the protonation mechanism. Essentially no deuterium is incorporated into the (trimethylsilyl)methylidene ligand in the $Cp^*_2Ru_2(\mu\text{-}CHSiMe_3)(\mu\text{-}O_2CCF_3)(\mu\text{-}Cl)$ product, as shown by ^1H, ^2H, and ^{13}C NMR studies. As suggested above, this result unambiguously shows that protonation occurs at a ruthenium center and not at the methylene carbon; furthermore, the result rules out all mechanisms that involve at any point the intermediacy of a ruthenium methyl complex formed by migration of a Ru—H ligand to the methylene group. Whereas formation of **4** proceeds via protonation at ruthenium, reductive elimination of $HSiMe_3$, and coordination by $O_2CCF_3^-$, formation of **5** proceeds via protonation at ruthenium, re-formation of the C—Si bond, α-hydrogen elimination, loss of H_2, and coordination by $O_2CCF_3^-$ (although not necessarily in that order).

Several different scenarios could account for the conversion of **1** to the methylene complex **4** at low temperature, but to a mixture of **4** and the (trimethylsilyl)methylidene complex **5** at room temperature. One possibility is that **4** and **5** are the result of the protonation of *different* species in solution (Scheme 3): **4** could be formed via the protonation of methylene complex **1** itself, while **5** could be formed via protonation of the $Cp^*_2Ru_2(\mu\text{-}CH_2SiMe_3)(\mu\text{-}Cl)$ intermediate thought to be responsible for the formation of mononuclear CH_2SiMe_3 and chloro complexes when **1** is treated with Lewis bases. Generation of the (trimethylsilyl)methylidene product **5** only at room temperature could be a consequence of the higher equilibrium concentration of $Cp^*_2Ru_2(\mu\text{-}CH_2SiMe_3)(\mu\text{-}Cl)$ and the preferential protonation of this intermediate at 25 °C. An alternative possibility is that, at some point in the protonation sequence, a common intermediate partitions between α-silyl elimination or α-hydrogen elimination pathways and that the branching ratio is temperature-dependent.

Scheme 3. Proposed Involvement of a (Trimethylsilyl)methyl Intermediate in the Reactions of 1 with Trifluoroacetic Acid

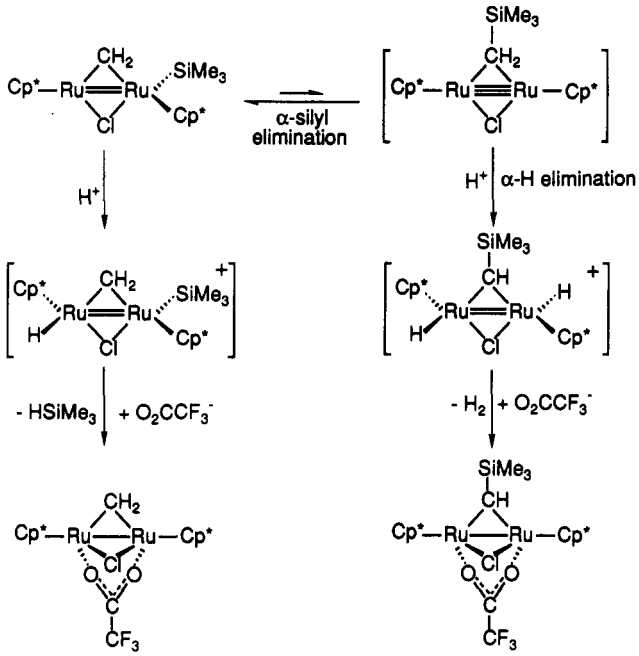

Synthesis of Cationic Bridging Alkylidene Complexes. In the previous section, we described the synthesis of two new alkylidene complexes; unlike the methylene/silyl complex **1**, the new alkylidene compounds **4** and **5** are *not* involved in dynamic processes that regenerate alkyl ligands. Consequently, addition of Lewis bases to **4** and **5** should not result in cleavage of the Ru—Ru bond and formation of mononuclear products. This expectation was confirmed by the following experiments.

Treatment of $Cp^*_2Ru_2(\mu\text{-}CH_2)(\mu\text{-}O_2CCF_3)(\mu\text{-}Cl)$ (**4**) with PMe_3 in toluene gives the new cationic methylene complex $[Cp^*_2Ru_2(\mu\text{-}CH_2)(PMe_3)(\mu\text{-}Cl)][O_2CCF_3]$ (**6**), in which the bridging trifluoroacetate ligand has been displaced. Although the (trimethylsilyl)methylidene complex **5** does not react in toluene with PMe_3, the same reaction carried out in dichloromethane gives the corresponding cation: $[Cp^*_2Ru_2(\mu\text{-}CHSiMe_3)(PMe_3)(\mu\text{-}Cl)][O_2CCF_3]$ (**7**).

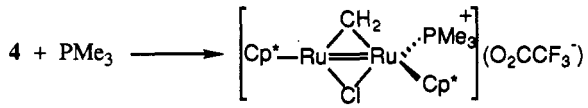

6

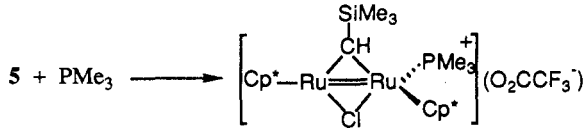

7

Salts analogous to 6 and 7 with the same cations but with $[H(O_2CCF_3)_2]$ counterions can be prepared directly from 1 by addition of excess HO_2CCF_3 and PMe_3 in the appropriate solvents.

The cationic alkylidene compounds 6 and 7 are both 1:1 electrolytes in nitrobenzene. The ionic nature of the trifluoroacetate group[60] is also evident from the IR spectra of 6 and 7, both of which contain a peak near 1700 cm^{-1}. The NMR spectra of 6 and 7 contain the characteristic deshielded ^1H and ^{13}C resonances for the alkylidene groups: these resonances appear near δ 10 and at δ 176.0 for 6 and at δ 13.15 and 202.9 for 7. There are two different Cp* environments in 6 and 7; in both complexes, the protons of *one* of the two Cp* groups are coupled to the ^{31}P nucleus of the trimethylphosphine ligand. These observations clearly establish that 6 and 7 are unsymmetric diruthenium complexes bridged by the alkylidene and chloride groups while the PMe_3 ligand is a terminal group on one of the ruthenium atoms. In fact, the structure of 6 closely resembles that of the methylene/silyl complex 1, with the PMe_3 group in 6 occupying the same coordination site as the $SiMe_3$ group in 1.

None of the alkylidene complexes 4–7 is fluxional; for example, the NMR resonances of 6 remain sharp even at 160 °C. From the 1.05 ppm separation between the ^1H NMR resonances of the bridging CH_2 groups in 6, and from the 13.0 ppm separation between the ^{13}C NMR resonances of the Cp* ligands in 6, it can be concluded that if there are any processes that exchange the CH_2 protons or the Cp* groups, they must have activation free energies *greater* than 21 kcal/mol.

Fluxionality of the Methylene/Silyl Complex: A Final Word. The reversible migration of the silyl group to the methylene unit in $Cp^*_2Ru_2(\mu\text{-}CH_2)(SiMe_3)(\mu\text{-}Cl)$, which was initially suggested on the basis of the variable-temperature NMR spectra, is strongly supported by the isolation of mononuclear ruthenium CH_2SiMe_3 alkyl complexes upon treatment with Lewis bases and by the isolation of dinuclear ruthenium $CHSiMe_3$ alkylidene complexes upon treatment with acids. Conclusive evidence in support of the rapidity with which the C–Si bond in 1 is reversibly re-formed has been obtained from studies of the cationic alkylidene complex $[Cp^*_2Ru_2(\mu\text{-}CH_2)(PMe_3)(\mu\text{-}Cl)][O_2CCF_3]$, which lacks a $SiMe_3$ ligand.

The stereochemical rigidity of the cationic phosphine complex $[Cp^*_2Ru_2(\mu\text{-}CH_2)(PMe_3)(\mu\text{-}Cl)][O_2CCF_3]$ (6) even at 160 °C is in stark contrast to the highly dynamic behavior of 1, which is fluxional on the NMR time scale even at −50 °C. This methylene/phosphine complex is structurally and electronically analogous to $Cp^*_2Ru_2(\mu\text{-}CH_2)(SiMe_3)(\mu\text{-}Cl)$: viz., the PMe_3 ligand in 6 and the $SiMe_3^-$ ligand in 1 are isosteric and isoelectronic. If the fluxional processes observed for the methylene/silyl complex 1 did not involve the *direct* participation of the silyl group, it would be difficult to explain why exchange of the Cp* ligands and exchange of the CH_2 protons in 1 have small activation barriers, while the methylene/phosphine complex 6 undergoes no dynamic processes with a free energy of activation less than 21.0 kcal/mol. This comparison convincingly demonstrates that the fluxionality of 1 *must* involve the direct participation of the $SiMe_3$ group: it migrates reversibly between the two ruthenium centers in the low-temperature dynamic process, and migrates reversibly to the bridging methylene group in the high-temperature dynamic process. All of the other possible mechanisms to explain the fluxionality of 1 (see Scheme 1) can be ruled out, since they would also be operative in 6.

Experimental Section

All operations were carried out under vacuum or under argon. Solvents were distilled under nitrogen from sodium benzophenone (pentane, diethyl ether, and tetrahydrofuran), sodium (toluene), or calcium hydride (dichloromethane) immediately before use. $[Cp^*RuCl]_4$,[37,38] $Mg(CH_2SiMe_3)_2$,[62] and PMe_3 were prepared via literature methods.[63] Carbon monoxide (Matheson) was used as received. HO_2CCF_3 (Aldrich) was distilled and stored in a glass flask with Teflon seals. Dry trifluoroacetic acid-*d*, DO_2CCF_3 (Aldrich), was used as received. IR spectra were recorded on a Perkin-Elmer 599B infrared spectrometer as Nujol mulls between KBr salt plates. The ^1H NMR data were obtained on a General Electric GN-500 spectrometer at 500 MHz, on a General Electric QE-300 spectrometer at 300 MHz, or on a General Electric NB-300 spectrometer at 300 MHz. The ^{13}C NMR data were obtained on a General Electric GN-500 spectrometer at 125 MHz or on a General Electric NB-300 spectrometer at 75 MHz. The ^{31}P NMR data were recorded on a General Electric NB-300 spectrometer at 121 MHz. The ^2H NMR data were obtained on a General Electric NB-300 spectrometer at 46 MHz. The solid-state ^{13}C NMR data were recorded on a General Electric GN-300 WB instrument at 75.4 MHz (^{13}C) by using the cross-polarized magic angle spinning technique. Chemical shifts are reported in δ units (positive shifts to high frequency) relative to TMS (^1H, ^2H, ^{13}C) or 85% H_3PO_4 (^{31}P). Microanalyses were performed by the University of Illinois Microanalytical Laboratory. Solution electrical conductivities were measured with a YSI Model 35 conductance meter used in conjunction with a calibrated cell with a cell constant of 1.0.

Simulations of the dynamic NMR spectra were carried out using the program DNMR, which is available from the Quantum Chemistry Program Exchange. The rates of exhange as a function of temperature were determined from visual comparisons of experimental spectra with computed trial line shapes. The errors in the rate constants of ca. 5% were estimated on the basis of subjective judgments of the sensitivities of the fits to changes in the rate constants. The temperature of the NMR probe was calibrated using methanol (for low temperatures) and ethylene glycol (for high temperatures),[64,65] and the estimated relative error in the temperature measurements was 0.5 K. The activation parameters were calculated from the Eyring equation by using an unweighted linear least-squares procedure contained in the program Passage, which is available from Passage Software, Inc. The errors in the activation parameters were computed from error propagation formulas which we have described elsewhere.[66]

$Cp^*_2Ru_2(\mu\text{-}CH_2)(SiMe_3)(\mu\text{-}Cl)$ (1). To a suspension of $[Cp^*RuCl]_4$ (3.10 g, 2.85 mmol) in diethyl ether (200 mL) at 25 °C was added bis((trimethylsilyl)methyl)magnesium (4.4 mL of a 0.81 M solution in diethyl ether, 3.56 mmol). The solution turned dark red immediately. After the solution had been stirred for 2.5 h, the solvent was removed under vacuum. The residue was extracted twice with pentane (200 mL, 60 mL). The combined extracts were filtered, and the filtrate was concentrated to ca. 150 mL and cooled to −20 °C to yield dark red crystals of the product. Yield: 2.91 g (86%). IR (cm^{-1}): 1248 (w), 1234 (w),

(62) Andersen, R. A.; Wilkinson, G. *Inorg. Synth.* **1979**, *19*, 262–264.
(63) Luetkens, M. L., Jr.; Sattelberger, A. P.; Murray, H. H.; Basil, J. D.; Fackler, J. P., Jr. *Inorg. Synth.* **1989**, *26*, 262–264.
(64) Van Geet, A. L. *Anal. Chem.* **1970**, *42*, 679–680.
(65) Friebolin, H.; Schilling, G.; Pohl, L. *Org. Magn. Reson.* **1979**, *12*, 569–573.
(66) Morse, P. M.; Spencer, M. D.; Wilson, S. R.; Girolami, G. S. *Organometallics*, in press.

1221 (s), 1069 (w), 1021 (s), 826 (s), 723 (m), 667 (w), 654 (m), 612 (m), 463 (w).

Reaction of $Cp^*_2Ru_2(\mu\text{-}CH_2)(SiMe_3)(\mu\text{-}Cl)$ with PMe_3. To a dark red solution of **1** (0.134 g, 0.225 mmol) in diethyl ether (40 mL) was added trimethylphosphine (0.1 mL, 0.99 mmol) at room temperature. The solution turned light orange immediately. After the solution had been stirred for 1 h, the solvent was removed under vacuum. The residue was extracted into pentane (50 mL). The extract was filtered, and the filtrate was concentrated to ca. 10 mL and cooled to −20 °C to yield orange crystals of $Cp^*RuCl(PMe_3)_2$ (**2a**). Yield: 0.072 g (76%). $^{31}P\{^1H\}$ NMR (C_6D_6, 25 °C): δ 3.1 (s). IR (cm^{-1}): 1422 (w), 1298 (w), 1280 (m), 1063 (w), 1022 (w), 956 (s), 938 (s), 850 (m), 718 (m), 665 (m), 611 (w), 360 (vw).

The mother liquors from above were further concentrated to ca. 2 mL and cooled to −20 °C to give a mixture of orange needles of $Cp^*RuCl(PMe_3)_2$ and light yellow plates. The yellow plates of $Cp^*Ru(CH_2SiMe_3)(PMe_3)_2$ (**3a**) were separated by hand. $^{31}P\{^1H\}$ NMR (C_6D_6, 25 °C): δ 6.4 (s). IR (cm^{-1}): 1420 (m), 1300 (w), 1294 (m), 1276 (s), 1255 (w), 1235 (s), 1064 (w), 1025 (m), 972 (w), 952 (s), 932 (vs), 849 (vs), 822 (s), 741 (m), 729 (m), 706 (m), 696 (w), 669 (m), 662 (m), 610 (w), 601 (vw), 377 (w).

NMR-Tube Reaction of $Cp^*_2Ru_2(\mu\text{-}CH_2)(SiMe_3)(\mu\text{-}Cl)$ with PMe_3. To a solution of **1** (0.020 g, 0.034 mmol) in CD_2Cl_2 (0.8 mL) in an NMR tube at −78 °C was added PMe_3 (0.02 mL, 0.198 mmol), and the mixture was thoroughly shaken at −78 °C just before the NMR tube was inserted into the NMR spectrometer. ^1H and $^{31}P\{^1H\}$ NMR spectroscopy showed that **1** had been quantitatively converted into **2a** and **3a** at −78 °C instantaneously.

Reaction of $Cp^*_2Ru_2(\mu\text{-}CH_2)(SiMe_3)(\mu\text{-}Cl)$ with CO. A solution of **1** (0.35 g, 0.59 mmol) in diethyl ether (60 mL) was transferred to a Fischer–Porter bottle and treated with 6 atm of carbon monoxide. The pressure dropped to 3 atm after the solution had been stirred at room temperature for 1 h. The excess CO was vented, and the solvent was removed under vacuum. The residue was washed with pentane (60 mL) to afford a yellow solution and a yellow precipitate of $Cp^*RuCl(CO)_2$ (**2b**). IR (cm^{-1}): 2023 (vs), 1954 (vs, br), 1071 (vw), 1024 (s), 794 (vw), 718 (w), 580 (w), 556 (m), 511 (s), 477 (w), 462 (vw), 438 (m), 423 (w), 400 (w), 388 (w), 378 (w), 355 (vw).

The light yellow pentane solution from above was concentrated and cooled to −20 °C to afford a mixture of yellow microcrystals of $Cp^*RuCl(CO)_2$ and colorless prisms. The colorless prisms of $Cp^*Ru(CH_2SiMe_3)(CO)_2$ (**3b**) were separated by hand. IR (cm^{-1}): 2003 (vs), 1941 (vs, br), 1617 (w), 1251 (w), 1237 (m), 1068 (w), 1027 (m), 964 (m), 853 (s), 824 (s), 750 (w), 727 (w), 673 (m), 601 (w), 590 (w), 575 (m), 540 (w), 511 (m), 430 (w), 371 (w).

$Cp^*_2Ru_2(\mu\text{-}CH_2)(\mu\text{-}O_2CCF_3)(\mu\text{-}Cl)$ (4). To a solution of **1** (0.23 g, 0.38 mmol) in dichloromethane (50 mL) at −78 °C was added HO_2CCF_3 (0.04 mL, 0.5 mmol). The mixture was slowly warmed to room temperature over 2 h. The solvent was removed under vacuum, and the residue was extracted into pentane (60 mL). The extract was filtered, concentrated to ca. 10 mL, and cooled to −20 °C to afford a dark green-blue powder. Yield: 0.15 g (61%). Molar conductivity (nitrobenzene, 10^{-3} M): 1.2 Ω^{-1} cm^2 mol^{-1}. IR (cm^{-1}): 1642 (s), 1203 (s), 1188 (s), 1143 (s), 1022 (m), 915 (w), 858 (m), 779 (w), 732 (m), 452 (w).

$Cp^*_2Ru_2(\mu\text{-}CHSiMe_3)(\mu\text{-}O_2CCF_3)(\mu\text{-}Cl)$ (5). To a solution of **1** (0.332 g, 0.56 mmol) in toluene (60 mL) at ambient temperature was added HO_2CCF_3 (0.1 mL, 1.3 mmol), and the mixture was stirred for 15 min. Trimethylphosphine (0.2 mL, 1.97 mmol) was added to convert $Cp^*_2Ru_2(\mu\text{-}CH_2)(O_2CCF_3)Cl$ (which is a byproduct of the reaction) to the salt $[Cp^*_2Ru_2(\mu\text{-}CH_2)(PMe_3)Cl][O_2CCF_3]$, which is not soluble in pentane and can be separated from the desired product in the next step. After addition of PMe_3, the reaction mixture was stirred for an additional 45 min. The solvent was removed under vacuum, and the residue was extracted with pentane (100 mL). The extract was filtered, and the filtrate was concentrated to ca. 50 mL and cooled to −20 °C to afford black plates. Yield: 0.19 g (47%). Molar conductivity (nitrobenzene, 10^{-3} M): 0.7 Ω^{-1} cm^2 mol^{-1}. IR (cm^{-1}): 1635 (s), 1259 (w), 1238 (m), 1198 (s), 1189 (w), 1144 (s), 1021 (m), 857 (m), 844 (w), 821 (vw), 779 (vw), 731 (s), 670 (w), 621 (w), 458 (vw).

Reactions of **1** with DO_2CCF_3 both at −78 °C and at 25 °C were carried out in exactly the same way as described above for the preparations of **4** and **5**. The extent of deuterium incorporation in the products was monitored by integration of the ^1H NMR spectra, by integration of the ^2H NMR resonances, and by examination of the one-bond carbon–deuterium coupling patterns of the alkylidene carbon resonances in the ^{13}C NMR spectra. All of these experiments indicated that <10% of the CH_2 sites in **4** and about 5% of the α-$CHSiMe_3$ sites in **5** were deuterated when DO_2CCF_3 was used in place of HO_2CCF_3.

$[Cp^*_2Ru_2(\mu\text{-}CH_2)(PMe_3)(\mu\text{-}Cl)][O_2CCF_3]$ (6). To a solution of **4** (0.23 g, 0.38 mmol) in dichloromethane (40 mL) was added PMe_3 (0.2 mL, 1.97 mmol) at room temperature. The mixture was stirred for 1.5 h, and a dark purplish red solution was obtained. The solvent was removed under vacuum, and the resulting residue was washed with diethyl ether (70 mL) to afford a deep maroon powder. Yield: 0.19 g (70%). Molar conductivity (nitrobenzene, 10^{-3} M): 25.1 Ω^{-1} cm^2 mol^{-1}. $^{31}P\{^1H\}$ NMR (CD_2Cl_2, 25 °C): δ 5.4 (s). IR (cm^{-1}): 1695 (vs), 1283 (w), 1195 (s), 1153 (s), 1110 (s), 1020 (m), 958 (s), 860 (w), 813 (s), 797 (m), 730 (w), 715 (m), 674 (w).

$[Cp^*_2Ru_2(\mu\text{-}CH_2)(PMe_3)(\mu\text{-}Cl)][H(O_2CCF_3)_2]$ (6′). (Method 1). To a solution of **1** (0.11 g, 0.19 mmol) in toluene (40 mL) at ambient temperature was added HO_2CCF_3 (0.04 mL, 0.5 mmol), and the mixture was stirred for 15 min. Trimethylphosphine (0.15 mL, 1.48 mmol) was added, and the mixture was stirred for another 1 h. The solvent was removed under vacuum, and the residue was washed with pentane (40 mL). The residue was extracted with diethyl ether (60 mL), and the extracts were filtered, concentrated to ca. 40 mL, and cooled to −20 °C to afford deep maroon needles. Yield: 0.088 g (58%).

Method 2. To a solution of **1** (0.30 g, 0.51 mmol) in dichloromethane (60 mL) at ambient temperature was added HO_2CCF_3 (0.1 mL, 1.3 mmol). The solution turned dark blue immediately and was stirred for 30 min. Trimethylphosphine (0.15 mL, 1.48 mmol) was added, and the solution turned dark red slowly over 1 h. The solvent was removed under vacuum, and the residue was extracted with diethyl ether (90 mL). The extract was filtered, and the filtrate was concentrated and cooled to −20 °C to give deep maroon needles. Yield: 0.095 g (23%). Molar conductivity (nitrobenzene, 10^{-3} M): 23.5 Ω^{-1} cm^2 mol^{-1}. The NMR data of **6′** are exactly identical with those of **6**. IR (cm^{-1}): 1778 (m), 1738 (s), 1286 (w), 1259 (m), 1190 (s), 1132 (m), 1018 (m), 944 (m), 797 (m), 707 (m), 606 (w), 502 (w).

$[Cp^*_2Ru_2(\mu\text{-}CHSiMe_3)(PMe_3)(\mu\text{-}Cl)][O_2CCF_3]$ (7). To a solution of **5** (0.13 g, 0.18 mmol) in dichloromethane (30 mL) at ambient temperature was added PMe_3 (0.13 mL, 1.28 mmol). The solution was stirred at room temperature for 8 h. The solvent was removed under vacuum, and the dark residue was washed with diethyl ether (50 mL) to afford a sticky black powder. Yield: 0.09 g (63%). Molar conductivity (nitrobenzene, 10^{-3} M): 23.5 Ω^{-1} cm^2 mol^{-1}. $^{31}P\{^1H\}$ NMR (CD_2Cl_2, 25 °C): δ −8.9 (s). IR (cm^{-1}): 1695 (s), 1283 (m), 1242 (m), 1197 (m), 1147 (w), 1105 (w), 1020 (s), 960 (s), 858 (m), 790 (m), 715 (m), 669 (m), 624 (w), 580 (vw), 545 (vw).

$[Cp^*_2Ru_2(\mu\text{-}CHSiMe_3)(PMe_3)(\mu\text{-}Cl)][H(O_2CCF_3)_2]$ 7′. To a solution of **1** (0.30 g, 0.51 mmol) in dichloromethane (60 mL) at ambient temperature was added CF_3CO_2H (0.1 mL, 1.3 mmol). The solution turned dark blue immediately and was stirred for 30 min. Trimethylphosphine (0.15 mL, 1.48 mmol) was added, and the solution turned dark red slowly over a period of 1 h. The solvent was removed under vacuum, the residue was washed with diethyl ether (3 × 30 mL), and the resulting black powder was dried under vacuum. Yield: 0.151 g (33%). Molar conductivity (nitrobenzene, 10^{-3} M): 24.6 Ω^{-1} cm^2 mol^{-1}. The NMR data of **7′** are exactly identical with those of **7**. IR (cm^{-1}): 1782 (s, br), 1738 (s, br), 1304 (w), 1286 (m), 1254 (w), 1243 (m), 1194 (s), 1131 (s), 1070 (w), 1020 (m), 960 (s), 945 (w), 852 (m), 788 (m), 702 (m), 670 (w), 614 (w), 587 (w), 516 (w), 422 (w), 378 (w).

Crystallographic Studies.[67] Single crystals of $Cp^*_2Ru_2(\mu\text{-}CH_2)(SiMe_3)(\mu\text{-}Cl)$ (1) grown from pentane were mounted on glass fibers using Paratone-N oil (Exxon) and were immediately cooled to −75 °C in a nitrogen stream on the diffractometer. Standard peak search and indexing procedures gave rough cell dimensions, and the diffraction symmetry was supported by examinations of the axial photographs. Least-squares refinement using 25 reflections yielded the cell dimensions given in Table 3.

Data were collected in one quadrant of reciprocal space ($\pm h,+k,-l$). Systematic absences for $0k0$ ($k \neq 2n$) and $h0l$ ($h + l \neq 2n$) were consistent only with the space groups $P2_1/n$. The measured intensities were reduced to structure factor amplitudes and their esd's by correction for background, scan speed, and Lorentz and polarization effects. While corrections for crystal decay were unnecessary, absorption corrections were applied. The maximum and minimum transmission factors were 0.794 and 0.580, respectively. Systematically absent reflections were deleted, and symmetry-equivalent reflections were averaged to yield the set of unique data. Only those data with $I > 2.58\sigma(I)$ were used in the least-squares refinement.

The structure was solved by direct methods (SHELXS-86) and unweighted difference Fourier syntheses. The positions of the ruthenium, chlorine, and silicon atoms were deduced from an E-map. Subsequent difference Fourier calculations revealed the positions of the remaining non-hydrogen atoms. The hydrogen atoms were included in the refinement as fixed contributors in "idealized" positions with C–H = 0.96 Å. The quantity minimized by the least-squares program was $\sum w(|F_o| - |F_c|)^2$, where $w = 1.23/(\sigma(F_o)^2 + (pF_o)^2)$. The analytical approximations to the scattering factors were used, and all structure factors were corrected for both the real and imaginary components of anomalous dispersion. In the final cycle of least squares, all non-hydrogen atoms were independently refined with anisotropic thermal coefficients, and a common group isotropic thermal parameter was varied for the other hydrogen atoms. Successful convergence was indicated by the maximum shift/error of 0.015 in the last cycle. Final refinement parameters are given in Table 3. The largest peaks in the final difference Fourier map were in the vicinity of the ruthenium atoms. A final analysis of variance between observed and calculated structure factors showed a slight dependence on $\sin\theta$.

(67) For a description of the crystallographic methods and programs employed, see: Jensen, J. A.; Wilson, S. R.; Girolami, G. S. *J. Am. Chem. Soc.* **1988**, *110*, 4977–4982.

Acknowledgment. We thank the Department of Energy (Grant DEFG02-91ER45439) for support of this research and Teresa Prussak-Wieckowska for assistance with the X-ray structure determination. We thank Dr. Zhehong Gan for assistance with the CPMAS study. W.L. thanks the Department of Chemistry at the University of Illinois for a fellowship, and G.S.G. acknowledges receipt of a Henry and Camille Dreyfus Teacher-Scholar Award (1988–1993).

Supplementary Material Available: Tables of calculated hydrogen atom coordinates and all bond distances and angles for 1 (6 pages). Ordering information is given on any current masthead page.

OM940023K